Available online at www.sciencedirect.com
SCIENCE DIRECT®
Journal of Molecular Catalysis A: Chemical 234 (2005) 121–127
JOURNAL OF MOLECULAR CATALYSIS A: CHEMICAL
www.elsevier.com/locate/molcata

A quantum-chemical study of CO adsorption on small Cu particles supported on reduced SiO_2

Ricardo M. Ferullo, Norberto J. Castellani *

Grupo de Materiales y Sistemas Catalíticos, Departamento de Física, Universidad Nacional del Sur, Av. Alem 1253, 8000 Bahía Blanca, Argentina

Received 3 January 2005; received in revised form 8 March 2005; accepted 8 March 2005
Available online 18 April 2005

Abstract

The adsorption of CO over monomer, dimer and trimer of copper deposited on a ≡Si–O• defect on silica surface was studied using the density functional theory formalism (DFT). The results indicate that the CO adsorption strength follows this order: Cu1 > Cu2 ≥ Cu3. With respect to the CO vibrational frequencies, whereas for closed-shell systems ($Cu1/SiO_2$, $Cu3/SiO_2$ and Cu_2O) the CO molecule shows, in comparison with free CO, the lower frequency shifts, for the open-shell system ($Cu2/SiO_2$) it produces the higher frequency shift. This behavior could be related with the variation of polarizabilities due to the interaction of CO with Cu_n/SiO_2. The signal at 2130 cm^{-1} experimentally observed for reduced Cu/SiO_2 catalysts could be assigned to the CO adsorption on a partially electropositive atomic Cu linked to a ≡Si–O• site.

Keywords: CO adsorption; Cu/SiO_2; Small Cu particles; Metal-support interaction; Density functional theory

1. Introduction

Cu-based catalysts are used for a variety of reactions such as methanol synthesis, oxidation of hydrocarbons and hydrogenation reactions [1–4]. The activity of these catalysts has also been examined for the catalytic reduction of NO_x [5,6] in automobile converters as a possible alternative facing supported Rh.

Numerous investigations of CO adsorption on different supported-Cu catalysts were performed using IR spectroscopy. The peak positions of CO adsorbed on copper have been found to fall in different regions according to its oxidation state (excluding Cu/zeolite systems): 2110 cm^{-1} and lower for Cu(0), 2110–2140 cm^{-1} for Cu(I) and 2145 cm^{-1} and above for Cu(II) [7]. This implies a frequency shift of −33 cm^{-1} and lower for Cu(0), −33 to −3 cm^{-1} for Cu(I) and +2 cm^{-1} and above for Cu(II), with respect to the gas phase molecule.

The presence of oxidized Cu species in reduced Cu/SiO_2 catalyst was reported by some authors. For instance, Kohler et al. [8] observed a band at 2175 cm^{-1} which they assigned to CO bound to isolated ionic Cu^+. This band did not vary in shape and position by reoxidation of the catalyst in N_2O; as a consequence, it would be an indication of the presence of an independent copper species incorporated in the silica surface.

Studying reduced Cu/SiO_2 catalysts, Boccuzzi et al. have recently ascribed a feature centered at 2130 cm^{-1} to CO adsorbed to isolated atoms or small two-dimensional copper particles partially electropositive by the interaction with the oxygen atom of the support [9]. This assignment could be done by comparing this band with a similar one at 2120–2130 cm^{-1} in Cu/TiO_2 catalysts which is present even after severe reductive treatments (up to 673 K) [10]. In this system the presence of partially electropositive copper was evidenced by UPS and EELS studies [11]. The almost completely isolated nature of these sites was clearly shown by using IR spectra of ^{12}CO–^{13}CO 1:1 mixtures [10]. Two adsorption bands with the same intensity were observed related to the two different isotopic species adsorbed on Cu surface sites. The very small intensity transfer at the maximum

* Corresponding author. Tel.: +54 291 4595141; fax: +54 291 4595142.
E-mail addresses: caferull@criba.edu.ar (R.M. Ferullo), castella@criba.edu.ar (N.J. Castellani).

1381-1169/$ – see front matter © 2005 Elsevier B.V. All rights reserved.
doi:10.1016/j.molcata.2005.03.001

coverage and the lack of any frequency shift by decreasing the coverage were clear indications that no dipole–dipole coupling between the adsorbed CO was acting on the sample. In a recent work, Tøpsoe studied with FTIR the adsorption of CO on copper supported on ZnO, Al_2O_3 and SiO_2 taking into account the reducibility of Cu and the geometry of Cu particles [12]. For Cu on Al_2O_3 and SiO_2 they found, besides the typical bands of CO/Cu^0, a higher frequency band at 2139 cm^{-1} (on Al_2O_3) and 2132 cm^{-1} (on SiO_2) which could be originated from CO/Cu^+ species. Moreover two other bands at 2155 and 2103 cm^{-1} have been related to CO adsorbed on Cu^{2+} and coordinatively unsaturated Cu^+ species, respectively. Later on, Greeley et al. [13] studied theoretically using a periodic DFT method the adsorption of CO on Cu(1 1 1) at the presence of different chemical environments. They concluded that in a partially oxidized Cu surface blue shifts (≈30–50 cm^{-1}) of CO vibrational frequencies are predicted.

Strong changes in the electronic structure have been observed when a small metallic particle is supported on oxides. In this context, theoretical studies of the interaction between gas molecules and supported small metallic particles are essential to get an accurate description of adsorption processes and they constitute a very useful tool for the understanding of the catalytic activity of supported metal systems. At the present there are relatively few quantum-chemical works devoted to the interaction of metallic aggregates with oxides usually used as catalyst supports. Particularly, the Cu/SiO_2 system has been studied mainly by N. Lopez et al. [13–17]. These authors found that the regular sites of the silica surface are unreactive toward Cu atoms. In contrast, defect sites like ≡Si• and ≡Si–O• (the (≡) symbol indicates the three Si–O bonds) are very reactive and they are probably centers where the nucleation takes place [15]. Using Cu_n clusters (n = 1–5) they observed a partial electron transfer from the metal to the oxide, yielding to the formation of an electrostatic interaction between Cu clusters and the non-defective two-coordinated O atoms of the silica surface [16]. On the other hand, the adsorption properties of small Cu particles were analyzed using Cu/SiO_2 cluster models [17,18]. Indeed, in a previous study we investigated the adsorption of isocyanate (NCO) over atomic and dimer copper deposited on silica defects [18].

In this study a theoretical analysis of the CO adsorption on Cu_n (n = 1–3) particles supported on a defective site at the silica surface is performed in the framework of density functional theory (DFT). We have only considered the ≡Si–O• defect because this site have been postulated to be the most reactive according to different ab-initio calculations [15,18]. The goal of this work is to attain a qualitative understanding of the CO interaction with these electropositive Cu particles by considering the results of binding energies and vibrational frequencies.

2. Theoretical considerations and surface models

The calculations have been performed within the density functional theory using the hybrid B3LYP exchange-correlation functional [19] as implemented in the software package Gaussian 98 [20]. This method has been widely used for adsorption processes yielding reliable results both on oxides and metal clusters.

The SiO_2(1 1 1) surfaces were represented using a $Si_3O_4(OH)_6$ cluster following the ideal β-cristobalite structure (see Fig. 1). In the past, it was established that the bond formed between Cu and defect sites of the silica surface is very local and even small clusters describe properly the nature of the interaction [14]. In this case the silica surface was represented by a chain of three tetrahedrons, the ≡Si–O• defect being localized in the central one. The terminal oxygen atoms were saturated with hydrogens in order to eliminate spurious effects due to the dangling bonds. The geometric structure of the tetrahedrons was not relaxed in the optimization process. In particular, the Si–O and the O–H distances were set to 1.61 and 0.98 Å, respectively. The Cu_n aggregates and the adsorbed CO geometries were fully optimized, as well as the coordinates of oxygen atom of ≡Si–O• defect.

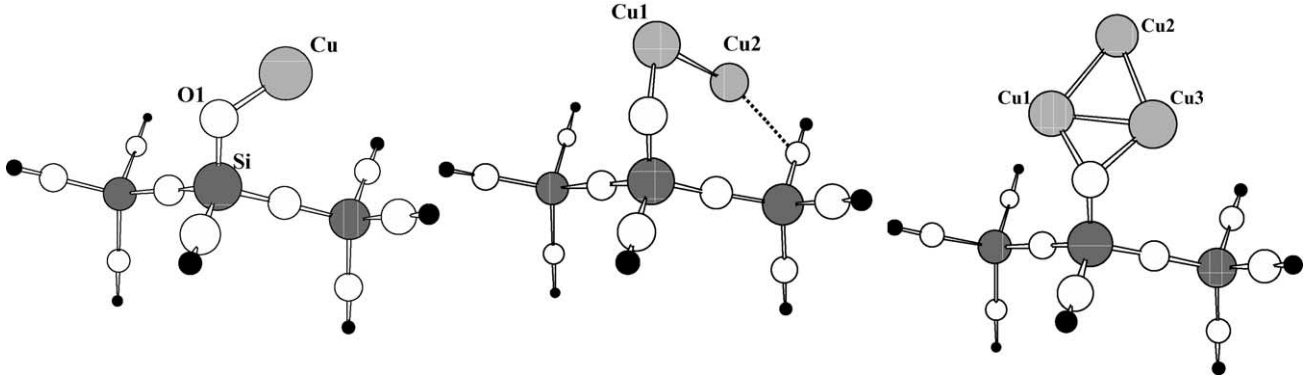

Fig. 1. Models of Cu monomer, dimer and trimer supported on a ≡Si─O· center at the silica surface. White spheres, oxygen atoms. O1 corresponds to the non-bridging oxgygen (surface defect), the other are bridging oxygens of the SiO_2 lattice. Dark grey spheres, silicon atoms. Light grey spheres, copper atoms. Small black spheres correspond to terminal hydrogen atoms.

The C, O and Si atomic orbitals were described with the all-electron 6–31 G basis set. For Cu, an effective core potential with a [8s5p5d/3s3p2d] basis set for the $3s^2 3p^6 3d^{10} 4s^1$ valence electrons was used [21]. Polarization functions were added to those atoms directly involved in the geometrical optimization. The atomic charges were calculated by using the natural bond orbital (NBO) population analysis [22].

The adsorption energies (E_{ads}) were calculated as the difference between the energy computed for the $CO/Cu_n/SiO_2$ system and the sum of energies for the separated fragments ($CO + Cu_n/SiO_2$). The full counterpoise procedure was applied to correct the basis set superposition error (BSSE) [23].

Vibrational frequencies have been computed by determining the second derivatives of the total energy with respect to the internal coordinates [24]. They were scaled according to a factor, calculated as the ratio between the empirical and the calculated free CO frequency values. The $\Delta\nu$ shifts are given with respect to free CO (for free CO a value of 2211 cm^{-1} was obtained).

3. Results and discussion

3.1. Copper clusters deposited on SiO_2 surface

As we have already mentioned, the adsorption of Cu particles on a silica ≡Si–O• defect was the object of several studies in the past by using cluster models within the DFT formalism [14–18]. In this section we will only discuss some of their relevant aspects (see Table 1). When the Cu particles interact with this defect an important electron transfer occurs from the metal to the support. The amount of this electron transfer is of 0.69, 0.65, 0.78e for copper monomer, dimer and trimer, respectively. The electronic charge taken by the support is mainly accumulated in the O atom of the ≡Si–O group. Indeed, the net charge of this atom (labeled O1 in the figures) changes from −0.59e in the defective bare surface to −1.2 or −1.3e when the Cu clusters interact with it. The Cu atoms directly linked to this O atom concentrate the positive charge for clusters Cu2 and Cu3. Moreover, for Cu2 only one Cu atom shears its chemical bonding with O1, while for Cu3 two Cu atoms participate on it. Then, we infer that the electron transfer increases with the number of Cu atoms linked to the defect and explain the variation of electron transfer as a function of Cu atoms in the cluster: this transfer would be nearly the same for Cu1 and Cu2, and increase for Cu3. The small decrease for Cu2 could be related to the presence of a competitive chemical interaction with a bridging O atom (see Fig. 1).

On the other hand, the corresponding Cu–O1 distance increases as the metal particle size increases. The adhesion energies, defined as $E_{adh} = [E(Cu_n/SiO_2) - E(Cu_n) - E(SiO_2)]$ with $n = 1$, 2 or 3, have also been computed. Notice that the E_{adh} values are higher for the Cu clusters with an odd-number of electrons (monomer and trimer). In these cases a strong covalent bond is produced by coupling the unpaired electron of these particles with that of the ≡Si–O• site.

The dimer adsorbs with the terminal Cu atom bended towards the surface. An electrostatic interaction occurs between this positively charged Cu atom and a regular bridging O atom, keeping at a distance of about 2.28 Å between them (Fig. 1). Although this interaction is absent for the adsorbed trimer, it was observed by López et al. for the Cu tretramer and pentamer [16].

The Cu3 trimer at gas phase presents a Jahn–Teller distortion resulting in a non-equilateral triangle with its largest angle having 74°. When this trimer interacts with the silica defect a quasi-equilateral triangle is formed with two Cu atoms interacting directly with the O atom of the support (Fig. 1).

The O atom of ≡Si–O• defect relaxes its position with respect that of a rigid lattice. Indeed, the Si–O1 distance show a slight stretching of 0.2 Å with respect to the bulk Si–O distance value.

3.2. CO adsorption on Cu_n/SiO_2 ($n = 1$–3)

In Tables 2–4 the main geometrical, electronic and energetic molecular properties are summarized for the CO adsorption on Cu1, Cu2 and Cu3 supported on silica, respectively. As comparison, the same properties for the Cu_n–CO ($n = 1$,

Table 1
Adhesion energies (eV), optimized distances (Å) and natural bond orbital (NBO) population analysis net charges (in electron units) for Cu atom, dimer and trimer adsorptions over a ≡Si–O• defect

	$Cu1/SiO_2$	$Cu2/SiO_2$	$Cu3/SiO_2$
E_{adh}	−2.83	−2.03	−3.80
d(Si–O1)	1.633	1.628	1.636
d(O1–Cu1)	1.807	1.839	2.002
d(Cu1–Cu2)	–	2.318	2.429
d(Cu1–Cu3)	–	–	2.386
d(Cu2–Cu3)	–	–	2.429
q(Si)	+2.48	+2.46	+2.49
q(O1)	−1.22	−1.22	−1.35
q(Cu1)	+0.69	+0.47	+0.52
q(Cu2)	–	+0.18	−0.26
q(Cu3)	–	–	+0.52

Table 2
Adsorption energies (eV), optimized distances (Å) and natural bond orbital (NBO) population analysis net charges (in electron units) for CO adsorption on supported and unsupported Cu atom

	$CO/Cu1/SiO_2$	CO/Cu1
E_{ads}	−1.51	−0.24
d(Si–O1)	1.628	–
d(O1–Cu)	1.767	–
d(Cu–C)	1.821	1.999
d(C–O)	1.139	1.151
q(Si)	+2.50	–
q(O1)	−1.27	–
q(Cu)	+0.74	+0.15
q(C)	+0.38	+0.29
q(O)	−0.40	−0.44

Table 3
Adsorption energies (eV), optimized distances (Å) and NBO net charges (in electron units) for CO adsorption on supported and unsupported Cu dimer

	$CO/Cu2/SiO_2$		CO/Cu2
	CO on Cu1	CO on Cu2	
E_{ads}	−0.90	−1.05	−0.50
d(Si−O1)	1.622	1.643	–
d(O1−Cu1)	1.807	2.002	–
d(O1−Cu2)	2.901	1.876	–
d(Cu−Cu)	2.546	2.512	2.270
d(Cu1−C)	1.850	–	1.943
d(Cu2−C)	–	1.848	–
d(C−O)	1.147	1.146	1.138
q(Si)	+2.47	+2.49	–
q(O1)	−1.25	−1.32	–
q(Cu1)	+0.68	+0.17	+0.24
q(Cu2)	+0.13	+0.66	−0.22
q(C)	+0.30	+0.32	+0.39
q(O)	−0.43	−0.42	−0.41

2, and 3) molecules at gas phase are included. The support can produce significant modifications on CO adsorption energy with respect gas phase clusters. This effect is important for the monomer where the magnitude of E_{ads} increases in 1.27 eV, while for the dimer it increases in 0.40 or 0.55 eV according to the Cu atom on which the adsorption takes place. On the other hand, the magnitude of E_{ads} for the trimer decreases in 0.70 eV when the terminal Cu3 atom is considered or it decreases very little (0.07 eV) in the case of the other Cu atoms of the triangle (Cu1 and Cu2).

CO adsorbs on the $Cu1/SiO_2$ system forming a linear O–Cu–C–O structure (Fig. 2). By comparing the supported and the unsupported systems we can observe in Table 2 that the interatomic distances Cu–C and C–O decrease in the presence of the SiO_2 support. The relatively high value of the adsorption energy (−1.51 eV) corresponds to a strong Cu–CO bond. Furthermore, notice that as a consequence of

Table 4
Adsorption energies (eV), optimized distances (Å) and NBO net charges (in electron units) for CO adsorption on supported and unsupported Cu trimer

	$CO/Cu3/SiO_2$		CO/Cu3
	CO on Cu1	CO on Cu2	
E_{ads}	−0.82	−0.19	−0.89
d(Si−O1)	1.635	1.632	–
d(O1−Cu1)	1.962	2.026	–
d(Cu1−Cu2)	2.634	2.484	2.370
d(Cu1−Cu3)	2.462	2.331	2.370
d(Cu2−Cu3)	2.344	2.472	2.461
d(C−Cu1)	1.875	–	1.895
d(C−Cu2)	–	2.484	–
d(C−O)	1.143	1.143	1.145
q(Si)	+2.50	+2.47	–
q(O1)	−1.35	−1.35	–
q(Cu1)	+0.66	+0.45	+0.35
q(Cu2)	−0.28	−0.03	−0.12
q(Cu3)	+0.46	+0.45	−0.12
q(C)	+0.35	+0.36	+0.31
q(O)	−0.43	−0.43	−0.42

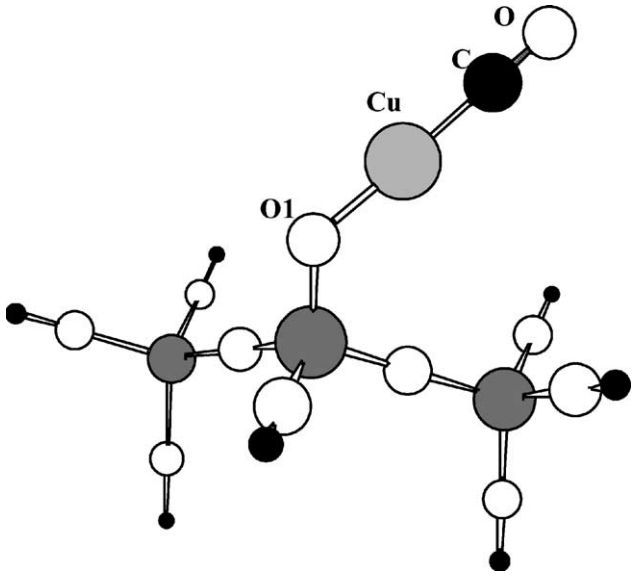

Fig. 2. Schematic representation of CO adsorption on silica-supported Cu1. The large black sphere corresponds to the carbon atom of CO.

the CO adsorption the Cu net charge varies slightly, from +0.69 (without CO) to +0.74e (with CO).

The CO adsorption on the supported-Cu2 were studied by positioning the CO molecule in the neighborhood of Cu atom directly linked with the support (Cu1 in Fig. 3) and near the terminal Cu atom (Cu2 in Fig. 3). In the former situation the geometry of the dimer does not change considerably. Conversely, when CO interacts with the formally terminal Cu atom, the above mentioned electrostatic interaction between this atom and the regular bridging O atom is broken and a strong covalent bond is established with the non-bridging O atom. Also in these cases a linear O–Cu–C–O structure results to be formed. According to the adsorption energies values shown in Table 3, CO adsorbs weakly on the supported dimer in comparison with the supported monomer.

The CO molecule adsorbs on the supported Cu3 on two different sites (Fig. 4). The stronger adsorption is produced when CO interacts with the Cu atom directly linked to support (Cu1). In this case an important distortion of the Cu3 ring is produced. The distances between Cu1 and the other copper atoms linked to it, Cu2 and Cu3, are elongated by 8.4 and 3.2%, respectively, with respect to the supported trimer without CO. On the other hand, the distance between Cu2 and Cu3 shortens by 5.5%. Due to an electron transfer from the trimer to the CO molecule, the Cu3 net charge increases slightly from +0.78 to +0.84. Also here the structure of the O–Cu–C–O group is quasi-linear. When CO adsorbs on the other possible adsorption site, Cu2, the distortion of the trimer geometry is less important. The Cu–Cu distances vary slightly, by about 2%. The large Cu–CO distance (2.027 Å) is by itself and indication of a weak adsorption. Indeed, the adsorption energy value (−0.19 eV) is much smaller in magnitude than when CO interacts with Cu1.

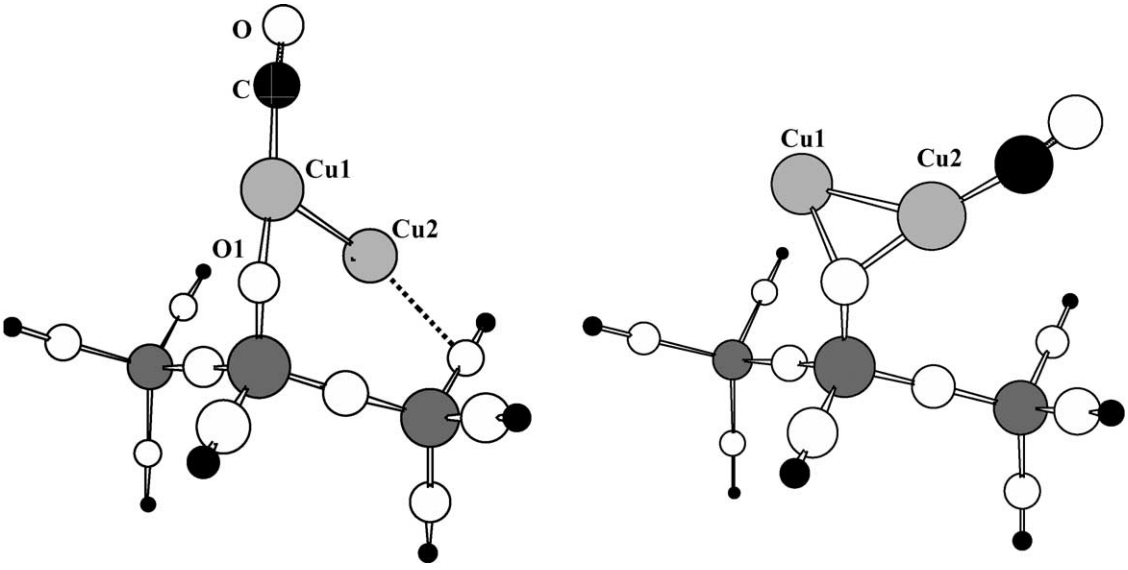

Fig. 3. Schematic representations of CO adsorption on silica-supported Cu2. The large black sphere corresponds to the carbon atom of CO.

As in the case of the Cu_n/SiO_2 systems the O atom of ≡Si–O• defect relaxes its position with respect that of a rigid lattice. The Si–O1 distance shows also a slight stretching (0.2–0.3 Å) with respect to the bulk Si–O distance value.

3.3. Analysis of the CO vibrational frequencies

In Table 5 the CO vibrational frequency values for the $CO/Cu_n/SiO_2$ systems are reported. For comparison reasons, the CO adsorption on $Cu_2O(1\,1\,1)$ surface were also considered and its corresponding CO stretching mode value was included in the same table. Indeed, the observed frequency value for CO on the surface of this oxide (2127 cm^{-1}) [25] is very close to that obtained on reduced Cu/SiO_2 (≈2130 cm^{-1}) [9,12]. The last frequency can be assigned to the CO interaction with partially positive small copper particles, as it was mentioned in the introduction. The $Cu_2O(1\,1\,1)$ surface was modeled using a $Cu_{16}O_8$ cluster (see Fig. 5). This cluster was embedded with an array of 78 point charges located at the ionic positions. Each Cu^+ ion was represented by a charge of +0.6e and an O^{2-} ion by a charge of −1.2e. These values are approximately the average NBO charges of Cu and O atoms in the cluster when the calculation was made without any embedding. Regarding the case of CO adsorbed on the supported monomer $Cu1/SiO_2$, we observe that also in this case the value of CO stretching mode is very close to that corresponding to reduced Cu/SiO_2 or Cu_2O. Therefore we could infer that in the works of Bocuzzi et al. [9] or Tøpsoe [12] the copper atoms are in an intimate contact with oxygen atoms.

The CO frequency shifts with respect to free CO (2143 cm^{-1}) downward in all the studied cases. It changes by

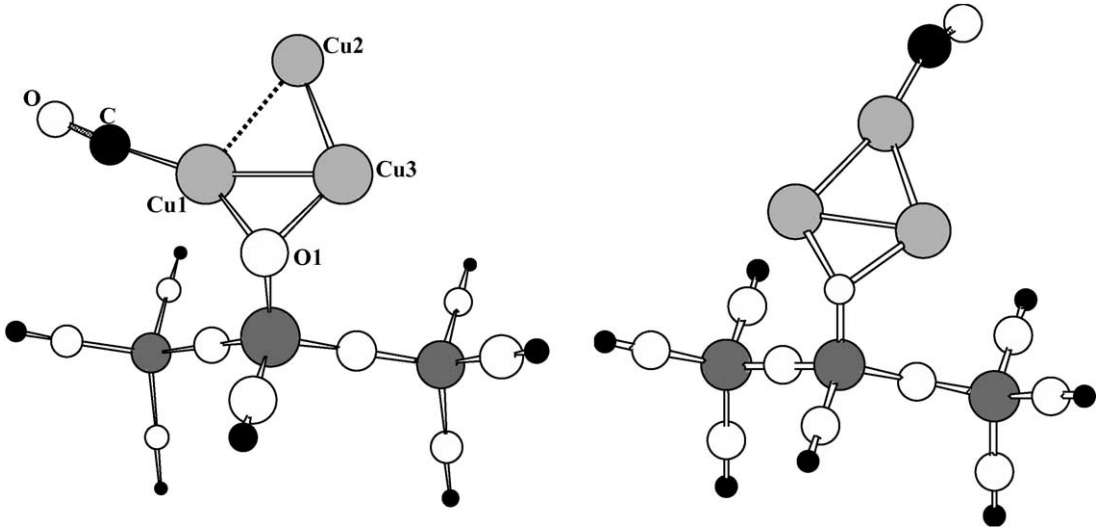

Fig. 4. Schematic representations of CO adsorption on silica-supported Cu3. The large black sphere corresponds to the carbon atom of CO.

Table 5
CO stretching frequencies (cm^{-1}) for the CO adsorption on supported monomer, dimer and trimer, and on the $Cu_2O(1\,1\,1)$ surface

	CO/Cu1/SiO_2	CO/Cu2/SiO_2		CO/Cu3/SiO_2		CO/Cu_2O
		CO on Cu1	CO on Cu2	CO on Cu1	CO on Cu2	
ν(CO)	2139	2049	2056	2096	2071	2120
$\Delta\nu$	−4	−94	−87	−47	−72	−23

Scaled according to the factor of 0.9692, calculated as the ratio between the empirical and the calculated free CO frequency values (2143/2211). The $\Delta\nu$ shifts are given with respect to free CO (2143 cm^{-1}).

$-4\,cm^{-1}$ on Cu1/SiO_2, by $\approx -90\,cm^{-1}$ on Cu2/SiO_2 and by -47 or $-72\,cm^{-1}$ on Cu3/SiO_2 according to the metallic site. The corresponding change for the adsorption on $Cu_2O(1\,1\,1)$ is intermediate: $-23\,cm^{-1}$, and in good agreement with the experimental value ($-16\,cm^{-1}$) [25]. It is interesting to note that the frequency shifts for supported dimer and trimer fall in the range experimentally found for the on-top CO adsorption on metallic Cu ($\approx -60\,cm^{-1}$) [26].

In a recent article, Cao et al. [27] have studied the CO interaction with Cu_n clusters ($n = 2$–13) at gas phase using DFT. They analyzed the nature of this interaction by determining the mean differences in polarizabilities, defined as $\Delta\alpha = \alpha_{CunCO} - \alpha_{Cun} - \alpha_{CO}$. The $\Delta\alpha$ values for the odd-size copper clusters (Cu3, Cu5, etc.) were relatively higher than those of the even-size clusters (Cu2, Cu4, etc.). This is consistent with an open-shell delocalized electronic structure for the odd-size clusters and a closed-shell configuration for the even-size clusters. On the other side, for small Cu_n clusters ($n \leq 9$) a correlation between $\Delta\alpha$ values and the red-shift frequencies was observed: the higher the mean polarizabilities, the higher the red-shift frequency values. Both trends are also present in our calculations concerning supported-Cu particles. The closed-shell systems (Cu1/SiO_2, Cu3/SiO_2 and Cu_2O) show the lower frequency shifts, and the open-shell system (Cu2/SiO_2) has the higher frequency shift. Besides, among the closed-shell systems, those ones in which CO interacts with an isolated or quasi-isolated Cu atom (like in Cu1/SiO_2 and $Cu_2O(1\,1\,1)$, where the nearest distance between Cu atoms is about 3 Å) have lower values than when the Cu atom can interact with other Cu atoms (like in Cu3/SiO_2). The absence of neighbor Cu atoms for the former systems results in a more localized net charge. The corresponding electronic structure could be related to a lower polarizability and a relatively lower red-shift.

Then, according to our frequency results, the signal at $2130\,cm^{-1}$ experimentally observed for reduced Cu/SiO_2 catalysts could be assigned to atomic Cu linked to a paramagnetic O atom of the support. Besides, the relatively high adsorption energy calculated for Cu1/SiO_2 is in agreement with FTIR spectra obtained during CO adsorption on reduced Cu/SiO_2 catalysts. Indeed, only the feature at $2130\,cm^{-1}$ is present after 10 min by outgassing at 523 K [9].

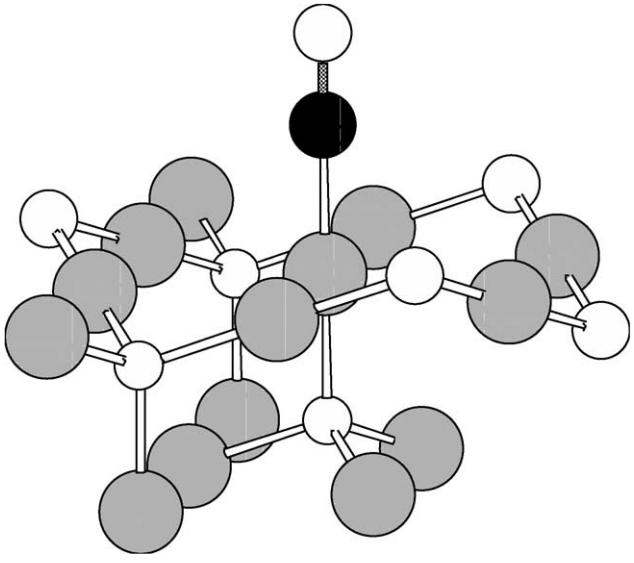

Fig. 5. CO adsorption on the $Cu_{16}O_8$ cluster representing the $Cu_2O(1\,1\,1)$ surface: white spheres, oxygen atoms; light grey spheres, copper atoms. The embedding of point charges is not shown. The large black sphere corresponds to the carbon atom of CO.

4. Conclusions

(i) The CO adsorption strength on supported Cu particules follows this sequence: Cu1 > Cu2 ≥ Cu3.
(ii) By comparing with the CO adsorption energy values for Cu clusters at gas phase we infer that the effect of the support is more important on the monomer (1.27 eV decrease) than on the dimer and trimer (0.40–0.55 eV decrease and 0.07–0.70 eV increase, respectively).
(iii) There is a general trend to form a linear O_{supp}–Cu–C–O structure.
(iv) For closed-shell systems (Cu1/SiO_2, Cu3/SiO_2 and Cu_2O) the CO molecule shows the lower frequency shifts, and for the open-shell system (Cu2/SiO_2) it produces the higher frequency shift. This behavior could be related with the different polarizabilities expected for CO–Cu/SiO_2.
(v) According to our results, the signal at $2130\,cm^{-1}$ experimentally observed for reduced Cu/SiO_2 catalysts could be assigned to the CO adsorption on atomic Cu linked to a paramagnetic O atom of the support.

Acknowledgements

Financial support from CONICET and UNS are gratefully acknowledged.

References

[1] D.B. Clarke, A.T. Bell, J. Catal. 154 (1995) 314.
[2] I.A. Fisher, A.T. Bell, J. Catal. 178 (1998) 153.
[3] S.C. Kim, J. Hazard. Mater. B91 (2002) 285.
[4] R.A. Koeppel, J.T. Wehrli, M.S. Wainwright, D.L. Trimm, N.W. Cant, Appl. Catal. A120 (1994) 163.
[5] Y. Chi, S.S.C. Chuang, J. Catal. 190 (2000) 75.
[6] T.W. Kim, M.W. Song, H.L. Koh, K.L. Kim, Appl. Catal. A210 (2001) 35.
[7] A. Dandekar, M.A. Vannice, J. Catal. 178 (1998) 621.
[8] M.A. Kohler, N.W. Cant, M.S. Wainwright, D.L. Trimm, J. Catal. 117 (1989) 188.
[9] F. Boccuzzi, S. Coluccia, G. Martra, N. Ravasio, J. Catal. 184 (1999) 316.
[10] F. Boccuzzi, A. Chiorino, G. Martra, M. Gargano, N. Ravasio, B. Carrozzini, J. Catal. 165 (1997) 129.
[11] M.C. Wu, P.J. Moeller, Surf. Sci. 224 (1989) 250.
[12] N.-Y. Tøpsoe, H. Tøpsoe, J. Mol. Catal. A: Chem. 141 (1999) 95.
[13] J. Greeley, A.A. Gokhale, J. Kreuser, J.A. Dumesic, H. Tøpsoe, N.-Y. Tøpsoe, M. Makrikakis, J. Catal. 213 (2003) 63.
[14] N. López, G. Pacchioni, F. Maseras, F. Illas, Chem. Phys. Lett. 294 (1998) 611.
[15] N. López, F. Illas, G. Pacchioni, J. Am. Chem. Soc. 121 (1999) 813.
[16] N. López, F. Illas, G. Pacchioni, J. Phys. Chem. B 103 (1999) 1712.
[17] N. López, F. Illas, G. Pacchioni, J. Phys. Chem. B 103 (1999) 8552.
[18] R.M. Ferullo, N.J. Castellani, J. Mol. Catal. A221 (2004) 155.
[19] A.D. Becke, J. Chem. Phys. 98 (1993) 5648.
[20] M.J. Frisch, G.W. Trucks, H.B. Schlegel, G.E. Scuseria, M.A. Robb, J.R. Cheeseman, V.G. Zakrzewski, J.A. Montgomery, R.E. Stratmann, J.C. Burant, S. Dapprich, J.M. Millam, A.D. Daniels, K.N. Kudin, M.C. Strain, O. Farkas, J. Tomasi, V. Barone, M. Cossi, R. Cammi, B. Mennucci, C. Pomelli, C. Adamo, S. Clifford, J. Ochterski, G.A. Petersson, P.Y. Ayala, Q. Cui, K. Morokuma, D.K. Malick, A.D. Rabuck, K. Raghavachari, J.B. Foresman, J. Cioslowski, J.V. Ortiz, B.B. Stefanov, G. Liu, A. Liashenko, P. Piskorz, I. Komaromi, R. Gomperts, R. L. Martin, D.J. Fox, T. Kieth, M.A. Al-Laham, C.Y. Peng, A. Nanayakkara, C. Gonzalez, M. Challacombe, P.M.W. Gill, B.G. Johnson, W. Chen, M.W. Wong, J.L. Andres, M. Head-Gordon, E.S. Replogle, J.A. Pople, Gaussian 98 Revision A.7, Gaussian Inc., Pittsburgh, PA, 1998.
[21] P.J. Hay, W.R. Wadt, J. Chem. Phys. 82 (1985) 299.
[22] A.E. Reed, L.A. Curtiss, F. Weinhold, Chem. Rev. 88 (1988) 899.
[23] N.R. Kestner, J.E. Combariza, in: K.B. Lipkowitz, D.B. Boyd (Eds.), Reviews in Computational Chemistry, vol. 13, Wiley-VCH, John Wiley and Sons Inc., New York, 1999, p. 99 (Chapter 2).
[24] M.M. Branda, C. Di Valentin, G. Pacchioni, J. Phys. Chem. B108 (2004) 4752.
[25] D. Scarano, S. Bordiga, C. Lamberti, G. Spoto, G. Ricchiardi, A. Zecchina, C. Otero Areán, Surf. Sci. 411 (1998) 272.
[26] K. Horn, J. Pritchard, Surf. Sci. 55 (1976) 701;
J.C. Cook, E.M. McCash, Surf. Sci. 356 (1996) L445.
[27] Z. Cao, Y. Wang, J. Zhu, W. Wu, Q. Zhang, J. Phys. Chem. B106 (2002) 9649.